
Supplementary information

Quantitative imaging of RNA polymerase II activity in plants reveals the single-cell basis of tissue-wide transcriptional dynamics

In the format provided by the
authors and unedited

Supplementary Information

S1 Calculations

S1.1 Incorporating a constant degradation rate into the calculation of total produced mRNA from microscopy

880 As noted by [9] and explained in Figure S5, the total number of transcripts produced by a locus can be obtained by integrating the area under the curve of a time trace of spot fluorescence. Here, we show how we incorporate mRNA degradation to estimate the mRNA abundance at a given time point.

885 The rate of change in mRNA, dM/dt , can be described by the sum of a production rate r and a degradation rate γ

$$\frac{dM}{dt} = \underbrace{r(t)}_{\text{change in mRNA}} - \underbrace{\gamma(t)M(t)}_{\text{production degradation}}. \quad (\text{S1})$$

As demonstrated by Bothma et al. [77] and Lammers et al. [17], the rate of mRNA production is proportional to the spot fluorescence. In addition, for the sake of simplicity we will assume that the degradation rate is constant. Hence, Equation S1 becomes

$$\frac{dM}{dt} = kFluo(t) - \gamma M(t), \quad (\text{S2})$$

where k is the proportionality constant between spot fluorescence and transcription rate. Equation S2 indicates that, to calculate the change in the number of mRNAs between two time points t and $t + \Delta t$, we need to know the number of mRNAs produced between these time points and subtract the number of mRNAs degraded. The mRNAs added between t and $t + \Delta t$, for time steps shorter than the transcriptional dynamics of the system are

$$\text{mRNA added} = \int_0^{t+\Delta t} Fluo(t) - \int_0^t Fluo(t) = \int_t^{t+\Delta t} Fluo(t), \quad (\text{S3})$$

which is equivalent to the sum of spot fluorescence values per frame up to time $t + \Delta t$ minus the sum up to time t . On the other hand, the number of mRNAs degraded between t and $t + \Delta t$ corresponds to the number of mRNAs at time t that decay with a rate γ (with units of time^{-1})

$$\text{mRNA degraded} = \gamma \times mRNA(t). \quad (\text{S4})$$

The change in mRNA from time t to $t + \Delta t$ is therefore

$$\text{mRNA change} = \text{mRNA added} - \text{mRNA degraded} \quad (\text{S5})$$

$$\text{mRNA change} = \int_t^{t+\Delta t} Fluo(t) - \gamma mRNA(t). \quad (\text{S6})$$

890 This formula was applied to spot fluorescence data to infer the total mRNA produced in Figure 2B and Figure 6B, F and G. Note that, to calculate averages across spots, it is necessary for their sampling times to be identical. This might not be the case when averaging across data sets due to sample adjustments during imaging, in which case the spot fluorescence traces were linearly interpolated to a rate of $\approx 7 \text{ s}$ per observation.

S1.2 Calculating the fluorescence intensity of a single RNAP molecule

895 In Figure 2D we show how we use nanocages to obtain the fluorescence calibration factor corresponding to a single GFP in fluorescence a.u. per molecule. Here, we explain how we use this number to calculate the fluorescence corresponding to a single actively transcribing RNAP molecule.

First, we consider that each RNAP is tethered to one nascent RNA, which contains 24 PP7 stem loop repeats, each repeat binding to an PCP-GFP dimer. For the sake of simplicity, we ignore RNAP molecules that have not completed transcription of the PP7 repeats since they contribute little to the overall signal (see below). Next, since each PP7 loop is bound by a PCP-GFP dimer, we multiply by a factor of two such that

$$\text{RNAP fluorescence} = \underbrace{0.078 \frac{\text{a.u.}}{\text{GFP}}}_{\text{GFP calibration}} \times \underbrace{24 \frac{\text{loops}}{\text{RNAP}}}_{\text{PP7 loops per RNA}} \times \underbrace{2 \frac{\text{GFP}}{\text{loop}}}_{\text{PCP per stem loop}} \approx 3.7 \frac{\text{a.u.}}{\text{RNAP}}, \quad (\text{S7})$$

where 0.078a.u./GFP corresponds to the GFP calibration obtained with nanocages as shown in Figure 2D. To convert spot fluorescence to number of RNAP molecules, we simply take the inverse of this result to obtain the number of RNAP molecules per arbitrary unit of fluorescence and multiply this value by the spot fluorescence value.

$$\text{RNAP per spot} = \frac{1}{3.7440} \frac{\text{RNAP}}{\text{a.u.}} \times \text{spot fluorescence a.u.} \quad (\text{S8})$$

In Figure 2E we show that the fluorescence of the dimmest spots (pink histogram) overlaps with that of their background fluctuations (green histogram) at approximately 10 a.u. . Applying Equation S8 we obtain the value of the dimmest detectable spots in terms of the number of RNAP molecules

$$\text{RNAP detection threshold} = \frac{1}{3.7440} \times 10 \approx 3. \quad (\text{S9})$$

We note that the number obtained from this calculation should be considered a slight underestimate because the RNAP molecules that have not finished transcribing the PP7 loops are not labeled with the full number of 48 GFP molecules. To estimate this error, we first consider an RNAP density on the reporter of ρ with units of $\frac{\text{RNAP molecules}}{\text{kbp}}$. We next define the number of RNAP molecules transcribing the PP7 loops N_{loops} as

$$\text{RNAP transcribing PP7 loops} = N_{loops} = \rho \times P \quad (\text{S10})$$

where P is the length of the PP7 loops in kbp. Similarly, we define N_{body} as the number of RNAP transcribing the rest of the gene body

$$\text{RNAP transcribing the rest of the gene} = N_{body} = \rho \times L \quad (\text{S11})$$

where L is the length of the reporter without considering the PP7 loops.

The RNAP molecules transcribing the loops have an increasing number of GFP molecules attached to them depending on how far into the PP7 loops they have transcribed. The last of the N_{loops} RNAP on the loops has a nascent RNA containing 23 loops and the one coming right before it has at most 22 loops, and so on. Considering that each loop binds a PCP-GFP dimer, then the total number of GFP molecules corresponding to RNAP molecules elongating the PP7 loops is

$$GFP_{pp7} = \sum_{i=1}^{N_{loops}} 2 \times \left[(i-1) \times \frac{23}{N_{loops}-1} \right] \quad (\text{S12})$$

where the square brackets symbolize the integer part of the number since the number of loops is discrete. We wish to estimate how this magnitude compares to the overall number of GFP molecules from all RNAP molecules actively transcribing the gene: N_{loops} plus N_{body} . The number of GFP in the rest of the gene is simply

$$GFP_{gene} = N_{body} \times 24 \times 2. \quad (\text{S13})$$

- 920 Thus, by plugging a realistic values of RNAP density ρ of up to 30 RNAP per kbp in Equations ?? through S13, the fraction of the signal corresponding to partially labeled RNAP molecules is given by

$$\frac{GFP_{pp7}}{GFP_{gene}} \approx 17\%, \quad (S14)$$

where we have used $P = 1.4$ kbp and $L = 5$ kbp.

- 925 We can also estimate how this partial labeling results in under-counting the number of RNAP molecules. We saw that there is a total of GFP_{pp7} GFP molecules labeling the RNAP that have not finished transcribing the PP7 loops. On the other hand, in our spot fluorescence calibration, all RNAP molecules are assumed to carry 48 GFP molecules (Eqn. S7). As a result, according to Equation S7 the number of RNAP on the PP7 repeats is estimated as $GFP_{pp7}/48$, which is clearly a larger number than N_{loops} . We can estimate the magnitude of this underestimation as the ratio 930 between the calibrated number of RNAP molecules assuming that partially labeled RNAP have 48 GFP, and the actual total number of RNAP on the reporter given by $N_{loops} + N_{body}$. Namely,

$$\text{Calibration underestimation} = \frac{\frac{GFP_{pp7}}{48} + N_{body}}{N_{loops} + N_{body}} \quad (S15)$$

The value of this expression is $\approx 85\%$ for realistic RNAP densities of up to 30 RNAP per kbp. This means that we underestimate the real number of RNAP transcribing the reporter (from beginning to end including the PP7 loops) by $\approx 15\%$ under steady-state conditions.

935 S1.3 Determining transgene copy number by qPCR

In this section, we present our calculation for determining the number of transgene insertions from the ΔCT values resulting from qPCR taking the amplification efficiency into account. Given a starting number of DNA molecules N_0 , the total number of molecules after C amplification cycles is given by

$$N(C) = N_0(2\epsilon)^C, \quad (S16)$$

- 940 where ϵ corresponds to the amplification efficiency, or the fraction of molecules that are duplicated in each cycle. The number of amplification cycles CT necessary to amplify the number of DNA molecules from N_0 to N_{ct} can be described by

$$CT = \log_{2\epsilon} \left(\frac{N_{ct}}{N_0} \right). \quad (S17)$$

Changing the logarithm base and rearranging leads to

$$CT = \frac{\log_2 \left(\frac{N_{ct}}{N_0} \right)}{1 + \log_2(E)}. \quad (S18)$$

We now define an amplification efficiency constant K as

$$K = \frac{1}{1 + \log_2(E)}. \quad (S19)$$

Equation S18 then becomes

$$CT = K \log_2 \left(\frac{N_{ct}}{N_0} \right). \quad (S20)$$

To experimentally obtain K (and therefore ϵ), we perform qPCR on serial dilutions of template DNA, thus varying N_0 . We then plot CT as a function of the \log_2 of the template concentration in order to obtain K from the slope (Fig. S10A,B). We used genomic DNA from a transgenic Arabidopsis plant to perform this amplification on the PP7 transgene as well as on an internal control genomic sequence. We measured both PCR reactions to have an efficiency of $K = 1$ within experimental

error. As a result, we can determine the ratio between the initial number of transgene molecules N_0^t and the initial number of internal control molecules N_0^c by calculating the ΔCT

$$\Delta CT = CT^t - CT^c = K \log_2 \left(\frac{N_{ct}}{N_0^t} \right) - K \log_2 \left(\frac{N_{ct}}{N_0^c} \right) = \frac{N_0^c}{N_0^t} \quad (\text{S21})$$

If the transgene occurs in a single insertion locus containing a single transgene copy per insertion, then in a T1 individual

$$\frac{N_0^c}{N_0^t} = 0.5, \quad (\text{S22})$$

which corresponds to a ΔCT value of -1. Using this approach we were able to identify transgenic Arabidopsis individuals with a single insertion locus containing a single transgene insertion (Fig. S10C).

S1.4 Decomposition of total variability into extrinsic and intrinsic noise

In this section we derive the formulas for the total, intrinsic and extrinsic noise (η_{tot}^2 , η_{int}^2 , and η_{ext}^2 , respectively) based on the two-reporter approach developed by Elowitz et al. [56]. As noted by Hilfinger et al.[78] and explained at length by Fu et al. [79], these expressions stem from the law of total variance, which states that, for a random output variable A and a random input variable X , the total variance of A can be decomposed as the sum

$$\underbrace{\text{Var}(A)}_{\text{total variance}} = \underbrace{\text{Var}_X(\langle A|X \rangle_A)}_{\text{explained variance}} + \underbrace{\langle \text{Var}_A(A|X) \rangle_X}_{\text{unexplained variance}}, \quad (\text{S23})$$

where the subscripts X or A indicate that the average or the variance is taken over different values of X or A , respectively.

Applied to the problem of gene expression variability, A represents the expression level of the gene of interest and X corresponds to the cellular state indicating, for example, the concentration in each given cell of all molecules that affect the expression of that gene such as RNAP. The first term on the right-hand side of Equation S23 is referred to as the *explained variance* and captures how much the average value of A varies across different values of X . The second term is referred to as the *unexplained variance* and captures how much the expression of A varies in cells that share the same value of X . See Figure S23 for a visual explanation of the law of total variance and Equation S23.

Because the identity and values of X are typically not known and/or not experimentally accessible, Elowitz et al. [56] devised a two-reporter system to determine the explained and unexplained components of the total normalized variance, which they termed extrinsic (η_{ext}^2) and intrinsic (η_{int}^2) noise, respectively. In this approach, each cell has two identical but distinguishable alleles of the gene of interest. In their statistical model, these two alleles are identical in all respects meaning that their distribution over cells and over time are the same. For the purpose of this derivation, let us call A_i and B_i the expression level of each allele in the i -th cell and normalize A and B to their means such that

$$\frac{A_i}{\langle A \rangle} = 1 + \delta A_i, \quad (\text{S24})$$

where δA_i is the fractional deviation of the expression level A_i from the mean $\langle A \rangle$. Similarly, for B we normalize to

$$\frac{B_i}{\langle B \rangle} = 1 + \delta B_i. \quad (\text{S25})$$

In the following calculations we will make use of the measurable quantities δA_i and δB_i to eliminate the unknown quantity X from Equation S23. We start by deriving an expression for η_{ext}^2 defined here as the explained component of the total variance of the normalized δA distribution

$$\eta_{ext}^2 = \text{Var}_X(\langle \delta A_i | X \rangle_A). \quad (\text{S26})$$

Note that, since X is a random variable, so is $\langle \delta A_i | X \rangle_A$, and we can write its variance as

$$\eta_{ext}^2 = \langle (\delta A_i | X)^2 \rangle_X - \langle \langle \delta A_i | X \rangle_A \rangle_X^2. \quad (S27)$$

Because both alleles are identical, $\langle \delta A_i | X \rangle_A$ is equal to $\langle \delta B_i | X \rangle_B$, which allows us to write Equation S27 as

$$\eta_{ext}^2 = \langle \langle \delta A_i | X \rangle_A \langle \delta B_i | X \rangle_B \rangle_X - \langle \langle \delta A_i | X \rangle_A \rangle_X \langle \langle \delta B_i | X \rangle_B \rangle_X. \quad (S28)$$

- 980 Note that, in this model, the variability in the values of A_i and B_i for cells with the same X are independent of each other since we assume that they are not explained by X . Because of this independence, $\langle A_i \rangle \langle B_i \rangle = \langle A_i B_i \rangle$ for a given X . Applied to the first term in Equation S28, the extrinsic noise can be written as

$$\eta_{ext}^2 = \langle \langle \delta A_i \delta B_i | X \rangle_{A,B} \rangle_X - \langle \langle \delta A_i | X \rangle_A \rangle_X \langle \langle \delta B_i | X \rangle_B \rangle_X. \quad (S29)$$

- We now note that the double angle brackets in the first term in the right-hand side of Equation S29 call for averaging the value of $\delta A_i \delta B_i$ in cells with the same X and then averaging again over all possible values of X . Similarly, the second term in the equation calls for averaging over A_i or B_i for a given X , and then averaging over X . This allows us to eliminate X in the equation and simplify our expression to

$$\eta_{ext}^2 = \langle \delta A \delta B \rangle - \langle \delta A \rangle \langle \delta B \rangle, \quad (S30)$$

which is the definition of covariance. Thus,

$$\eta_{ext}^2 = \text{Cov}(\delta A, \delta B). \quad (S31)$$

- 990 This makes intuitive sense, as the model assumes that, since A and B are identical genes that respond to X in the exact same way, the variance in the expression of A that is explained by X is identical to the variance in the expression of B that is explained by X . As a result, the extrinsic noise measures how A and B coordinately vary across cells.

- We now turn our attention to the derivation of the intrinsic noise, which we define as the unexplained component of the variance in the normalized A distribution, namely

$$\eta_{int}^2 = \langle \text{Var}_A(\delta A_i | X) \rangle_X. \quad (S32)$$

Replacing the unexplained variance in Equation S23 with η_{int}^2 , the explained variance by its formulation as extrinsic noise from Equation S31, and rearranging leads to

$$\eta_{int}^2 = \text{Var}(\delta A_i) - \text{Cov}(\delta A_i, \delta B_i). \quad (S33)$$

- Because this equation does not involve X we don't need the subscripts anymore: all variances are calculated across values of δA and δB . We now note that the total variance of δA and δB must be 1000 the same since they have the same distribution over cells and over time. Therefore we are allowed to express the first term in the right-hand side of Equation S33 as the average variance of the δA_i and δB_i distributions

$$\eta_{int}^2 = \frac{1}{2} [\text{Var}(\delta A_i) + \text{Var}(\delta B_i)] - \text{Cov}(\delta A_i, \delta B_i). \quad (S34)$$

Rearranging Equation S34 leads to

$$\eta_{int}^2 = \frac{1}{2} [\text{Var}(\delta A) + \text{Var}(\delta B) - 2\text{Cov}(\delta A, \delta B)]. \quad (S35)$$

- Now, using the identity stating that the variance of a sum is the sum of the variances minus twice their covariance, Equation S35 becomes

$$\eta_{int}^2 = \frac{1}{2} \text{Var}(\delta A_i - \delta B_i). \quad (S36)$$

Finally, we define the total noise η_{tot}^2 as the total variance of the normalized δA_i distribution. As noted before, because the distributions of δA_i and δB_i are identical, so are their variances. Therefore, the total noise can be calculated from the average

$$\eta_{tot}^2 = \frac{1}{2} [\text{Var}(\delta A_i) + \text{Var}(\delta B_i)], \quad (\text{S37})$$

which satisfies

$$\eta_{tot}^2 = \eta_{ext}^2 + \eta_{int}^2. \quad (\text{S38})$$

1010 Note that, here, we considered δA loosely as the “expression level” of gene A . This analysis can be applied to any metric of gene expression such as the instantaneous transcription rate, or the total amount of produced mRNA.

S2 Biological material

Plasmids			
Plasmid Name	Codes for	Function	Addgene
UPG	AtUBQ10p::PCP-mGFP5 (hyg resistance in plants)	Ubiquitous expression of PCP-GFP fusion	161003
UPmCh	AtUBQ10p::PCP-mCherry (hyg resistance in plants)	Ubiquitous expression of PCP-mCherry fusion	161004
UMsfG	AtUBQ10p::MCP-sfGFP (hyg resistance in plants)	Ubiquitous expression of MCP-sfGFP fusion	161005
AL13Rb	PP7-Gus-Luc AtUBQ10p::H2B-mScarlet (kan resistance in plants)	+ Promoterless PP7 reporter and red nuclear marker	161006
AL12R	AtUBQ10p::H2B-mScarlet + PP7-Gus-Luc (kan resistance in plants)	Promoterless PP7 reporter and Histone-mScarlet RFP nuclear marker	161007
AL13Rb-35S	35S-PP7 reporter in AL13Rb	Reports on 35S promoter activity and labels nuclei red	161008
AL13Rb-GAPC2	GAPC2-PP7 reporter in AL13Rb	Reports on Arabidopsis GAPC2 promoter activity and labels nuclei red	161009
AL12R-HSP70	HSP70-PP7 reporter in AL12R	Reports on Arabidopsis HSP70 promoter activity and labels nuclei red	161010
HSP70-pp7i-mCh-UPG	Arabiopsis HSP70 C-terminal mCherry fusion, intronic PP7	Reports on Arabidopsis HSP70 transcription activity and protein abundance	161011
AL13Rb-HsfA2	HsfA2-PP7 reporter in AL13Rb	Reports on Arabdiopsis HsfA2 promoter activity and labels nuclei red	161012
AL12R-EF-Tu	EF-Tu-PP7 reporter in AL12R	Reports on Arabidopsis EF-Tu promoter activity and labels nuclei red	161013
AL12R-HSP101	HSP101-PP7 reporter in AL12R	Reports on Arabdiopsis HSP101 promoter activity and labels nuclei red	161014

Table S1. List of Agrobacterium plasmids for expression in plants used in this study (continues on next page).

Plasmids			
Plasmid Name	Codes for	Function	Addgene
UtB2N7	AtUBQ10p::tagBFP2-NLS	Nuclear localized blue fluorescent protein marker	161015
UBC1cer60G	AtUBC1::60mer-mGFP5	Weak ubiquitous expression of an ER-targeted 60mer monomer fused to mGFP5	161016
UBC1cer120G	AtUBC1::mGFP5-60mer-mGFP5	Weak ubiquitous expression of an ER-targeted 60mer monomer fused to two mGFP5	161017
UBC1cer40GEM	AtUBC1::40nmGEM-mGFP5	Weak ubiquitous expression of an ER-targeted monomer of a 40nm GEM fused to mGFP5	

Table S1. Continued from previous page: List of Agrobacterium plasmids for expression in plants used in this study.

Arabidopsis Gene Identifiers		
Gene abbreviation	Gene name	AGI
UBQ10	Polyubiquitin 10	AT4G05320.2
H2B	Histone 2B	AT5G22880.1
GAPC2	Glyceraldehyde-3-phosphate dehydrogenase C2	AT1G13440.1
HSP70	Heat shock protein 70	AT3G12580.1
UBC1	Ubiquitin carrier protein 1	AT1G14400.1
HSP101	Heat shock protein 101	AT1G74310.1
HsfA2	Heat shock transcription factor A2	AT2G26150.1
EF-Tu	GTP binding Elongation factor Tu family protein	AT1G07920.1

Table S2. Arabidopsis gene identifiers of the genes used for the constructs in this study.

Arabidopsis lines generated in this study		
Name	Transgenes (refer to the 'Plasmids' table)	Usage
UPG-6	UPG	For transformation with reporter constructs
UPG-9	UPG	For transformation with reporter constructs
AL13Rb-35S	UPG and AL13Rb-35S	Image 35S promoter activity in Figure 1
AL12R-HSP101-1	UPG and AL12R-HSP101	Image AtHSP101 promoter activity in Figures 2 to 6
AL13Rb-HSP101-2	UPG and AL13Rb-HSP101	Image AtHSP101 promoter activity in Figure 6
AL13Rb-HSP101-3	UPG and AL13Rb-HSP101	Image AtHSP101 promoter activity in Figure S20
AL13Rb-HsfA2-1	UPG and AL13Rb-HsfA2	Image AtHsfA2 promoter activity in Figures 3 and 5
AL13Rb-HsfA2-2	UPG and AL13Rb-HsfA2	Image AtHsfA2 promoter activity in Figure 6
AL13Rb-HsfA2-3	UPG and AL13Rb-HsfA2	Image AtHsfA2 promoter activity in Figure S20
AL12R-EF-Tu-1	UPG and AL12R-EF-Tu	Image AtEF-Tu promoter activity in Figures 3, 5 and Fig. S6
AL12R-EF-Tu-2	UPG and AL12R-EF-Tu	Image AtEF-Tu promoter activity in Figures S20

Table S3. List of transgenic Arabidopsis lines used for experiments.

S3 Supplementary Figures

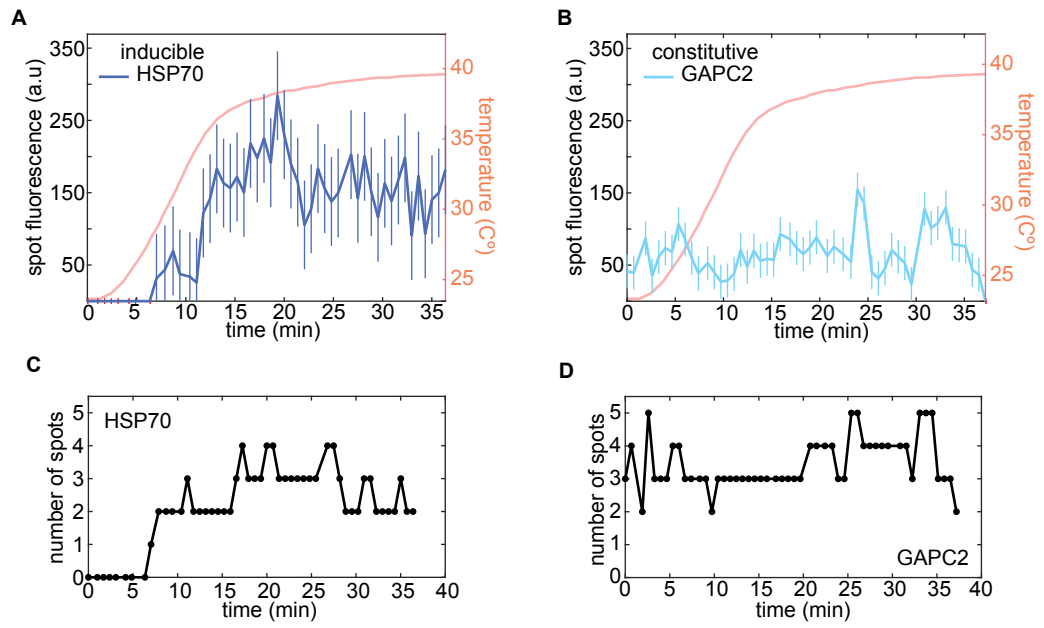


Figure S1. Related to Figure 1D and E. Additional transcription spots in tobacco show the same qualitative transcriptional dynamics. (A) HSP70-PP7 fluorescence time trace of a second transcription spot in the same nucleus as in Figure 1E. (B) GAPC2-PP7 fluorescence time trace of a second spot in the same nucleus as in Figure 1E. (C) Number of spots as a function of time in the nucleus shown in Figure 1D, left. (D) Number of spots as a function of time in the nucleus shown in Figure 1D, right. Error bars in (A) and (B) correspond to the uncertainty of spot fluorescence estimation based on their background fluctuations as described in Materials and Methods.

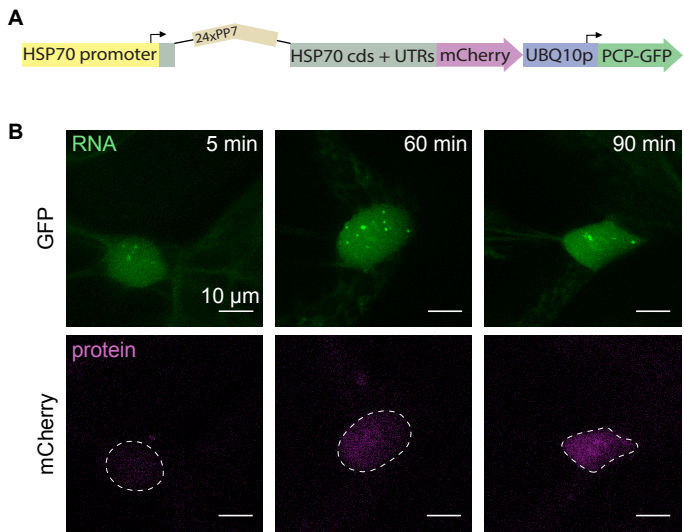


Figure S2. Related to Figure 1. Simultaneous imaging of transcriptional activity and protein product in tobacco. **(A)** Schematic of the construct used where the PP7 cassette is inserted into an intron in the Arabidopsis *HSP70* gene, which is fused in its C-terminus to mCherry. The same plasmid encodes a ubiquitously expressed PCP-GFP fusion. **(B)** Maximum fluorescence projection snapshots of a tobacco cell expressing the construct in (A) under heat shock. Nuclear mCherry fluorescence increases over time, consistently with the reported nuclear localization of HSP70 family proteins in plants [80].

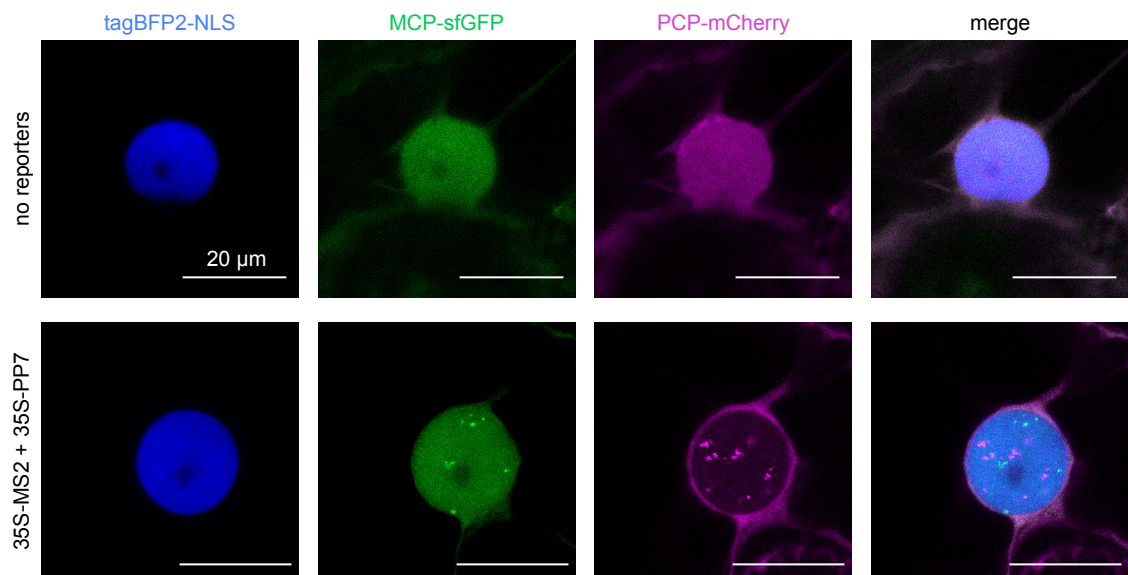


Figure S3. Related to Figure 1F. MCP-sfGFP and PCP-mCherry are homogeneously distributed in the nucleus in the absence of transcription. Maximum fluorescence projection snapshot of the nucleus of a tobacco cell expressing MCP-sfGFP, PCP-mCherry and nuclear localized tagBFP2. No nuclear puncta appear in the absence of PP7 and MS2 reporters.

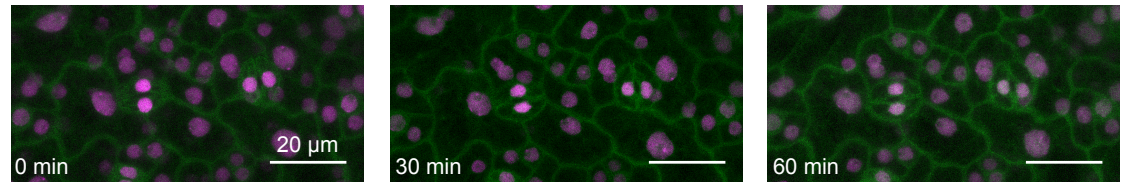


Figure S4. Related to Figure 2A. Lack of HSP101 induction at room temperature. Maximum z-projected image snapshots of the PCP-GFP/HSP101-PP7 Arabidopsis line imaged at room temperature. No spots were detected after continuous imaging for 60 minutes. Scale bar = 20 μ m.

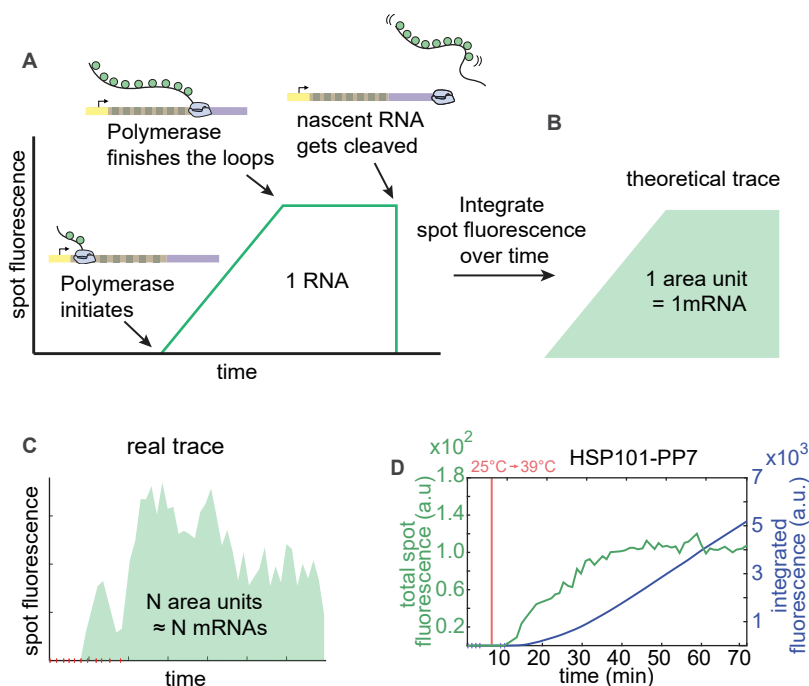


Figure S5. Related to Figure 2B. Integrated fluorescence as a metric for total mRNA produced. (A) Fluorescence profile of a single RNAP molecule as it traverses the gene. (B) Integrating this curve over time yields a unit of area associated with the production of a single mRNA molecule. (C) In the case of an actual transcription spot—resulting from the activity of multiple polymerase molecules—the integrated fluorescence over time will correspond to a number of area units equal to the number of produced mRNA molecules. (D) Data from a HSP101-PP7 replicate from Figure 2. Total spot fluorescence normalized by the number of cells in the field of view (green) and time integral of this signal (blue). The red horizontal line indicates when the stage temperature was shifted from room temperature to 39°C.

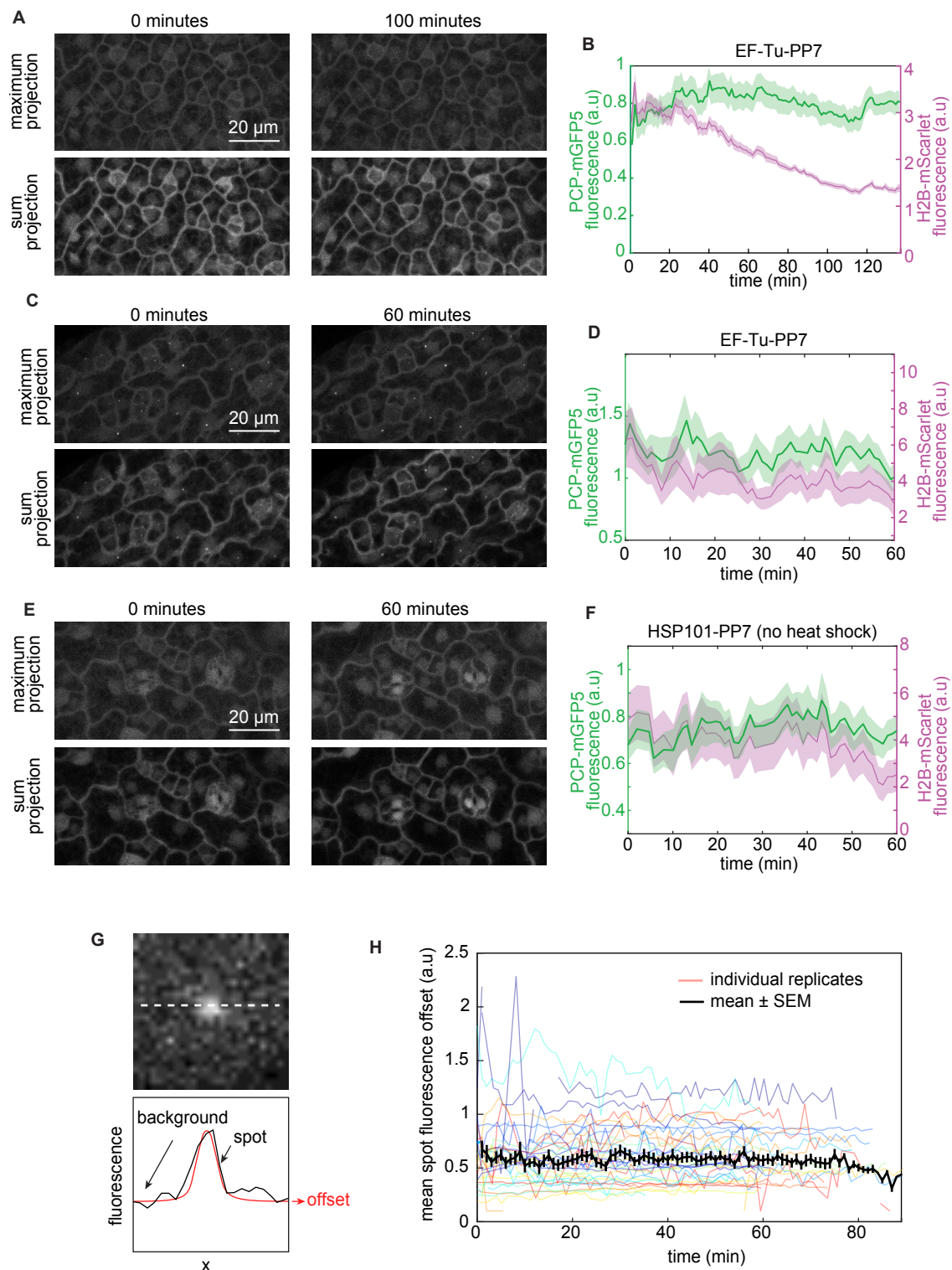


Figure S6. Related to Figure 2B. Absence of GFP photobleaching during time lapse experiments. (A) Snapshots of the PCP-GFP channel in leaves of an *Arabidopsis* plant carrying a constitutively expressed EF-Tu-PP7 reporter at the beginning of the experiment (left) and after 100 minutes of imaging (right). Two types of z-projections are shown: maximum projection (top) and sum projection (bottom). (B) Mean nuclear fluorescence in the GFP and the mScarlet channel in the movie shown in (A) ($n=48$ nuclei per frame). See Materials and Methods: Image analysis: nucleus fluorescence for details on nuclear fluorescence measurements. (C) Same as (A) in a second EF-Tu-PP7 line. Caption continues on next page.

Figure S6. Continued from previous page: Absence of GFP photobleaching during time lapse experiments. **(D)** Mean nuclear fluorescence in the GFP and mScarlet channels in the movie shown in (C) ($n=26$ nuclei per frame). **(E)** Same as (A) in uninduced plant carrying HSP101-PP7. **(F)** Mean nuclear fluorescence in the GFP and mScarlet channels in the movie shown in (E) ($n=29$ nuclei per frame). In (A)-(F) Nuclear PCP-GFP levels remain relatively stable, ruling out that photobleaching is affecting measurements of mRNA production. **(G)** Schematic showing how the spot fluorescence offset is calculated (for details see Materials and Methods: Spot fluorescence and tracking). On top, a maximum projection snapshot of a transcription spot. The dashed line indicates one of the dimensions along which fluorescence is calculated. At the bottom, the fluorescence profile along this line is used to fit a Gaussian curve (red). The baseline of the Gaussian corresponds to the spot fluorescence offset shown in (H). **(H)** Mean spot fluorescence offset over time in all the movies included in this study (colored lines) and mean spot fluorescence offset across all movies (black line). The background fluorescence, measured as spot offset, is stable over 60 minutes of continuous imaging, indicating that PCP-GFP is not being photobleached at an appreciable level. In (B), (D) and (F) the shaded areas correspond to the SEM over nuclei. In (H) the error bars correspond to the standard error across movies. In (A), (C) and (E) the same brightness and contrast setting were used to display the images corresponding to both time points.

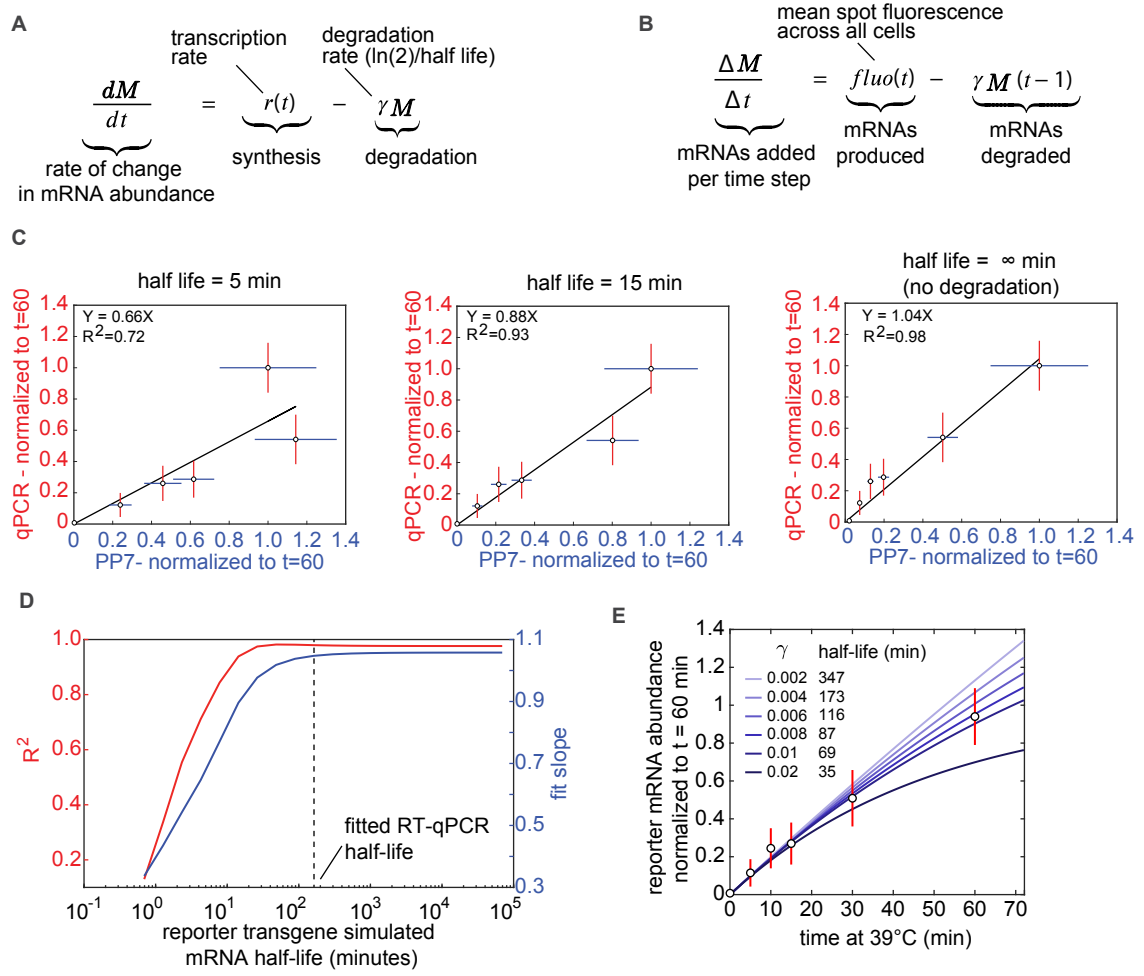


Figure S7. Related to Figure 2B. Exploring the effect of the mRNA degradation rate on the validation of the PP7 system against RT-qPCR measurements. (A) The rate of change in mRNA abundance is determined by a time-dependent rate of mRNA synthesis $r(t)$ and a constant mRNA degradation rate γ . (B) Discretized version of equation (A) used to obtain the accumulated mRNA based on spot fluorescence measurements. At each time point, the rate of synthesis is equal to the spot fluorescence while the number of mRNA molecules accumulated up to the previous time point are degraded at a simulated rate γ . Note that the mRNA half-life is defined as $\tau_{1/2} = \ln(2)/\gamma$. (C) Linear regression between the reporter mRNA abundance measured by RT-qPCR versus microscopy as in Figure 2C using the equation in (B) to incorporate mRNA degradation into the microscopy-based measurement. Because microscopy only reports on the synthesized, not the degraded, mRNA, we considered different, constant degradation rates and included this correction in the linear regression. (D) Fit parameters (R^2 and fit slope) as shown in (C) were calculated for a range of mRNA degradation rates expressed as half-lives. There is a good correlation and a constant slope between RT-qPCR and microscopy for half-lives longer than ~ 10 minutes. The dashed horizontal line indicates the fitted reporter mRNA half-life obtained in (C). (E) The reporter mRNA abundance measured by RT-qPCR was fitted to the mRNA accumulation model in (A) assuming a constant synthesis rate. mRNA accumulation according to RT-qPCR is almost linear on the timescales tested, resulting in a relatively long half-life. This half-life value is within the regime where there is a good correlation between PP7 fluorescence and qPCR (see vertical dashed line in (D)). Error bars in (C) and (E) correspond to the SEM across $n=3$ biological replicates in the case of RT-qPCR and $n=8$ biological replicates in imaging experiments. For details about these calculations see Section S1.1.

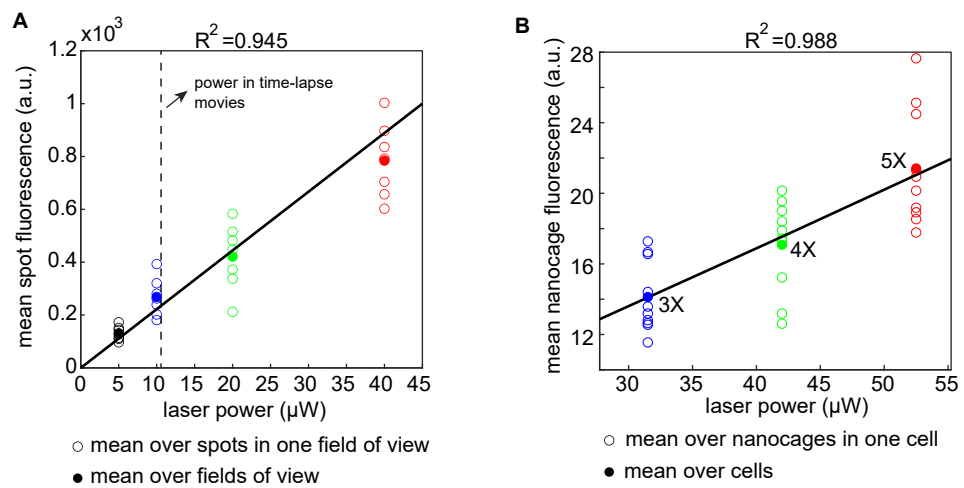


Figure S8. Related to Figure 2: The fluorescence intensity of PP7 transcription spots and 60mer nanocages is linear with laser power intensity. (A) Mean spot fluorescence of PP7 transcription spots driven by the constitutive EF-Tu promoter as a function of laser power intensity. Open circles correspond to the mean of all spots in a single snapshot in one field of view. Filled circles correspond to the mean taken over the mean of each snapshot. The vertical dashed line indicates the laser power used in time-lapse experiments. The solid black line corresponds to a linear fit to the data going through the origin, with $R^2 = 0.945$. (B) Mean fluorescence of 60mer GFP nanocages in tobacco cells as a function of laser power intensity. Open circles correspond to the mean nanocage fluorescence in one cell. Filled circles indicate the mean over the mean of each cell. The black solid line corresponds to a linear fit to the data going through the origin, with an R^2 value of 0.988. Shown next to each mean value is how much stronger the laser power is compared to the power in time-lapse experiments (3, 4 or 5 times stronger).

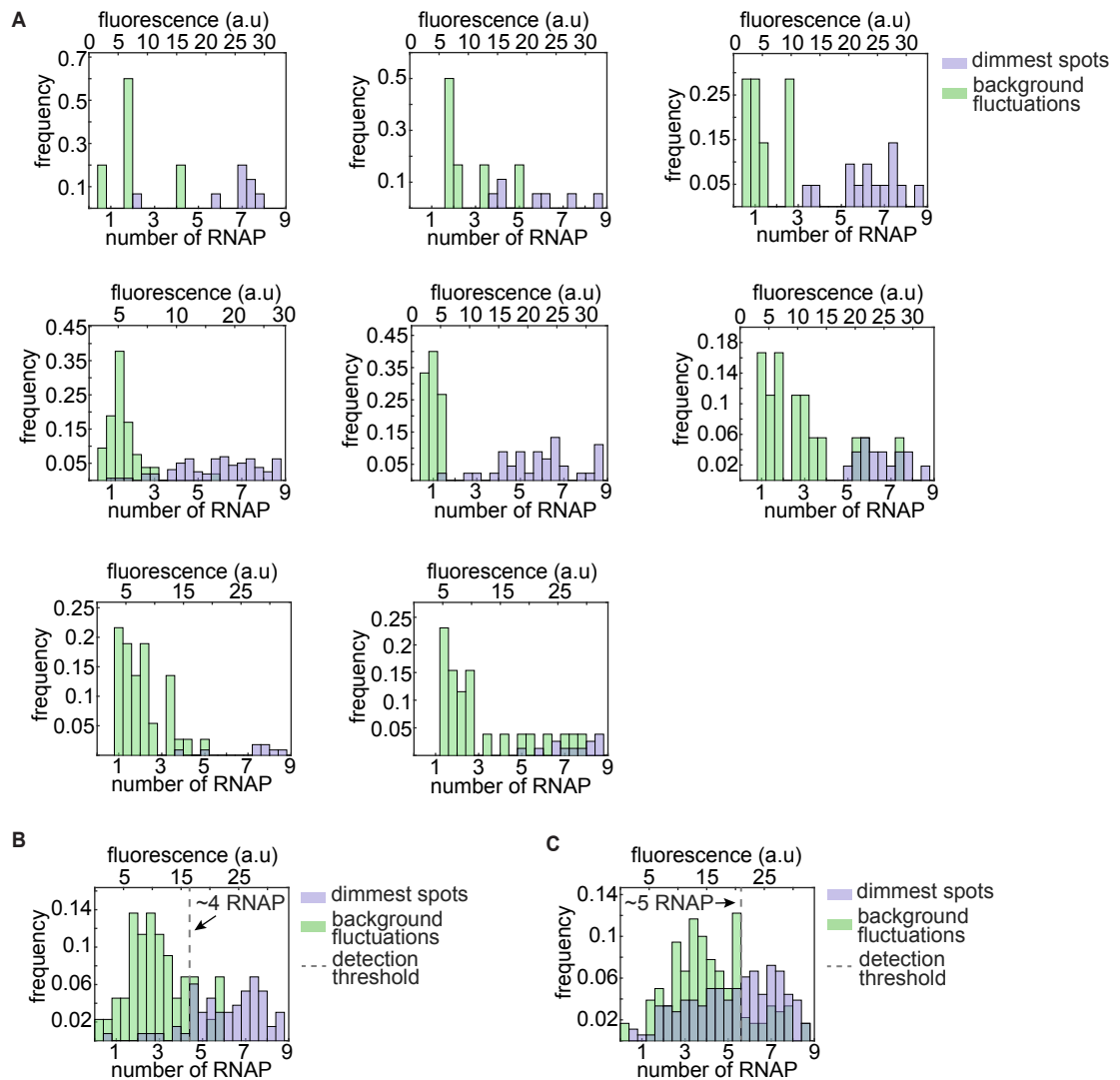


Figure S9. Related to Figure 2E. Detection threshold analysis in individual HSP101-PP7 replicates and different reporters. **(A)** Histograms of the calibrated number of transcribing RNAP molecules in the dimmest three frames of the weakest half of HSP101-PP7 fluorescence time traces (blue) and their associated fluorescence background fluctuations (green) as in Figure 2E. Each panel corresponds to an individual HSP101-PP7-1 replicate. **(B)** Same as (A) and Figure 2E where all the HsfA2-PP7-1 replicates were pooled together. **(C)** Same as (A) and Figure 2E where all the EF-Tu-PP7-1 replicates were pooled together. Note that, due to larger background fluctuations, the estimated detection threshold in (B) and (C) is larger than that of HSP101-PP7 shown in Figure 2E. This is likely due to a slightly higher PCP-GFP concentration in these lines.

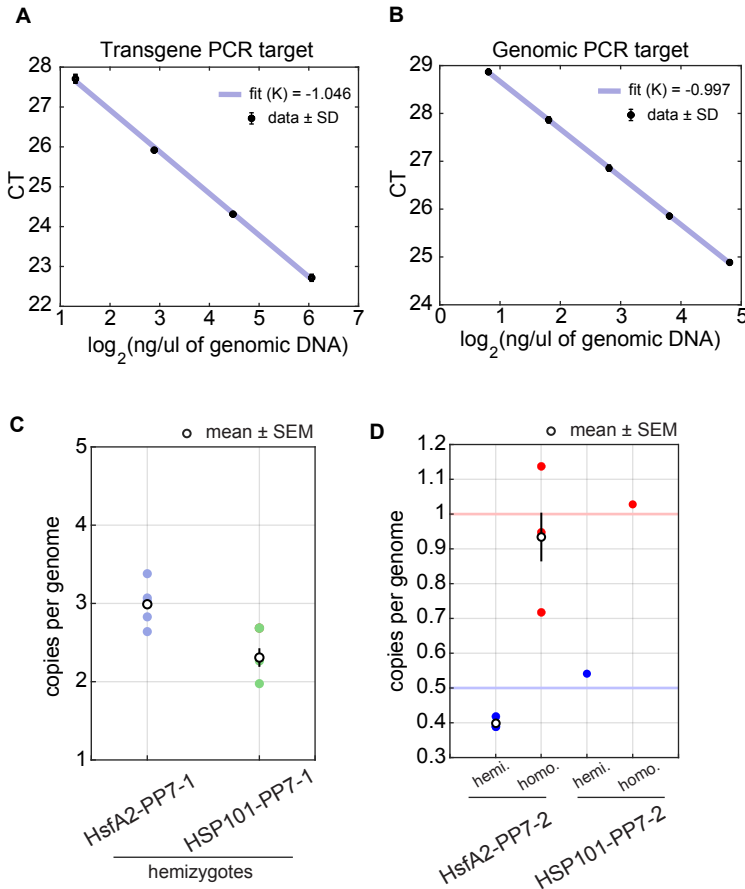


Figure S10. Amplification efficiency of primer pairs and determination of the copy number of single insertion lines. (A) qPCR results for serial dilutions of HSP101-PP7-2 Arabidopsis plants using primer pairs targeting the reporter transgene. (B) Same as (A) for a primer pair targeting a genomic location upstream of the *Lhcb3* gene that we use to determine the CT value corresponding to one genomic copy. In (A) and (B), the slope of the linear fit corresponds to $K = 1/(1 + \log_2(\epsilon))$ where ϵ is the amplification efficiency. (C) Number of copies of the PP7 reporter transgene per genome copy in hemizygous individuals of HSP101-PP7-1 and HsfA2-PP7-1. (D) Number of copies of the PP7 reporter transgene per genome copy in two single insertion reporter lines in hemizygous and homozygous individuals. The horizontal blue line indicates the expected value for a single-copy hemizygous plant where the insertion locus contains a single copy of the transgene. The red horizontal line indicates the expected value for a plant homozygous for a single insertion where this insertion contains a single copy of the transgene. Error bars in (C) and (D) correspond to the SEM across n=3 biological replicates.

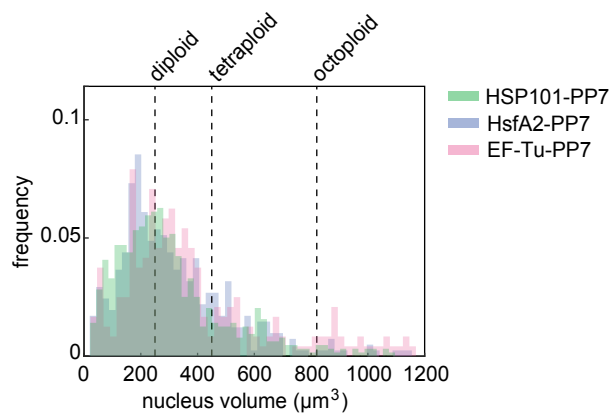


Figure S11. Related to Figure 3. Nuclear volume distribution. Histograms showing the volume of all nuclei in all the datasets included throughout this study. The nuclear volume was estimated by fitting maximum projections of the nuclear Histone-mScarlet channel to ellipsoids to obtain the major and minor axes for each nucleus. Shown on top are the mean nucleus volume of cells with different ploidy levels in *Arabidopsis* sepals according to [36].

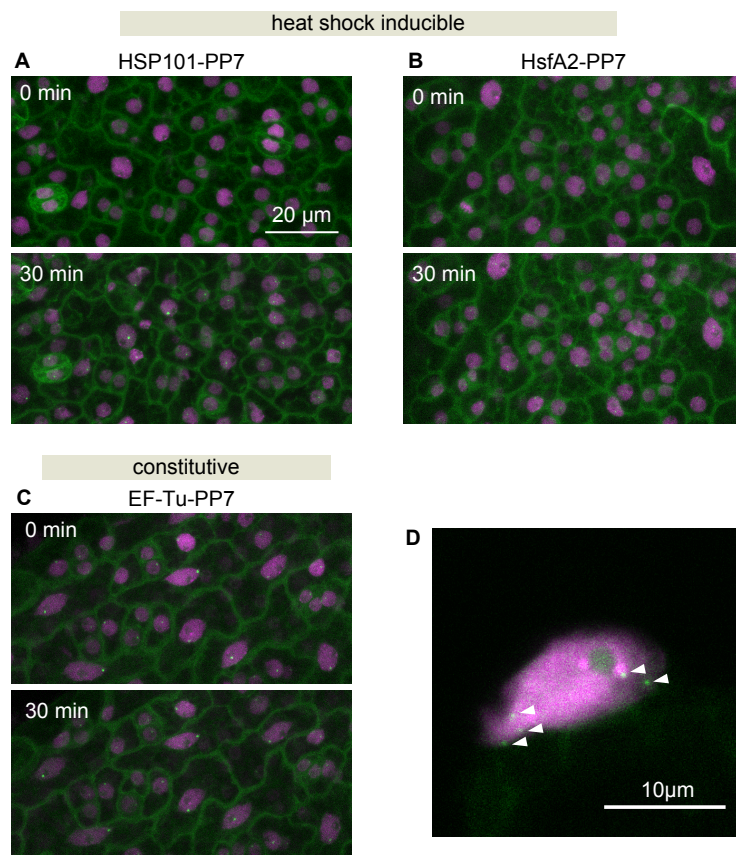


Figure S12. Related to Figure 3B: Young diploid cells in hemizygous single insertion lines have a single spot per nucleus. Polyploid cells display multiple spots. (A) Maximum projection snapshot of epidermis tissue near the base of the leaf from PCP-GFP Arabidopsis hemizygous for a single insertion of HSP101-PP7. On top, the sample at the beginning of a heat shock experiment. At the bottom, the same field of view after 30 minutes at 39°C. The PCP-GFP channel is shown in green, the Histone-mScarlet channel is shown in magenta. (B) Same as (A) but with HsfA2-PP7 instead of HSP101-PP7. (C) Plant hemizygous for a single insertion of a constitutively expressed EF-Tu-PP7 reporter at room temperature. Note that in (A)-(C), each nucleus has at most one transcription spot. (D) Polyploid Nucleus in a fully mature leaf from the plant in (B). White arrowheads indicate multiple transcription spots.

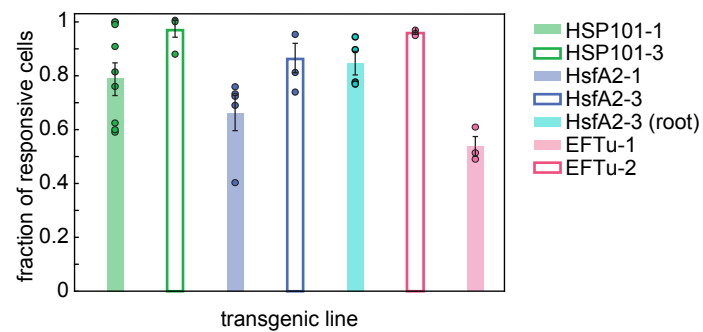


Figure S13. Related to Figure 3A. Reproducibility of the fraction of responsive cells. Mean fraction of transcriptionally responsive cells, defined as the number of nuclei that display reporter activity at least in one time point during the experiment divided by the total number of nuclei in the field of view (see Fig. 3A, bars on the right of each heat map). Circles represent single biological replicates (i.e movies). Error bars correspond to the SEM across n = 8, 4, 5, 4, 4, 3, and 4 biological replicates of HSP101-PP7-1, HSP101-PP7-3, HsfA2-PP7-1, HsfA2-PP7-3, HsfA2-PP7-3 (roots), EFTu-PP7-1, and EFTu-PP7-2, respectively.

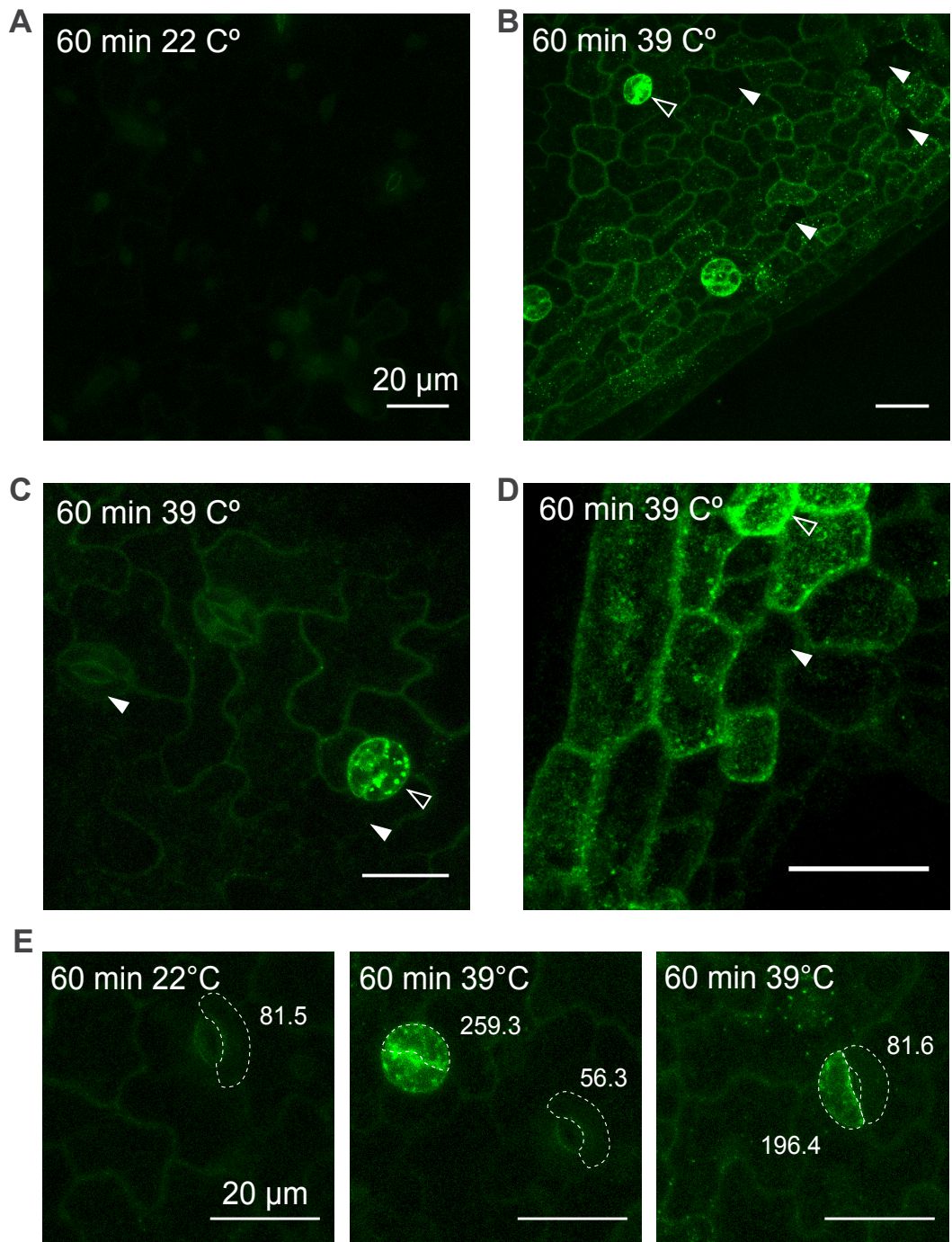


Figure S14. Related to Figure 3: A rescue construct of HSP101-GFP reveals how refractory cells lead to substantial cell-to-cell heterogeneity in HSP101-GFP accumulation upon heat shock. (A-E) Maximum fluorescence projections of leaf epidermis cells from *hsp101* knockout mutant plants complemented with a transgene coding for a HSP101-GFP fusion driven by 734 bp of the endogenous HSP101 promoter [40]. Detached leaves were treated with 39°C or 22°C for 60 minutes prior to imaging. (A) Untreated control. (B-D) Treated samples. White filled arrowheads indicate cells with negligible levels of GFP accumulation. Empty white arrowheads indicate cells with high levels of GFP accumulation. (E) Quantification of GFP fluorescence in treated and untreated cells. The dashed line highlights cells whose fluorescence was calculated. The numbers next to each cell correspond to the integrated GFP fluorescence of the volume of each cell highlighted.

A Spatially random distribution (hypergeometric)

$$\text{probability of } k \text{ active nuclei out of } n \text{ closest neighbors} = \frac{\binom{K}{k} \binom{N-K}{n-k}}{\binom{N}{n}}$$

K = number of active nuclei in field of view

k = number of active closest neighbors

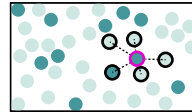
N = number of nuclei in field of view

n = number of closest neighbors

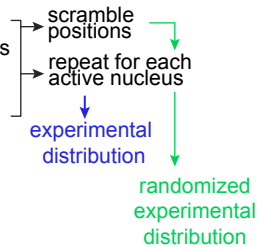
B N = 39 K = 11



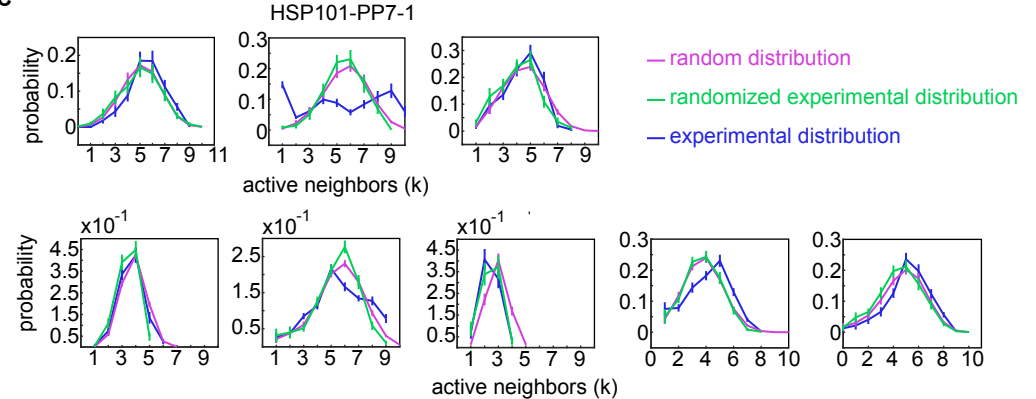
n = 5 k = 1



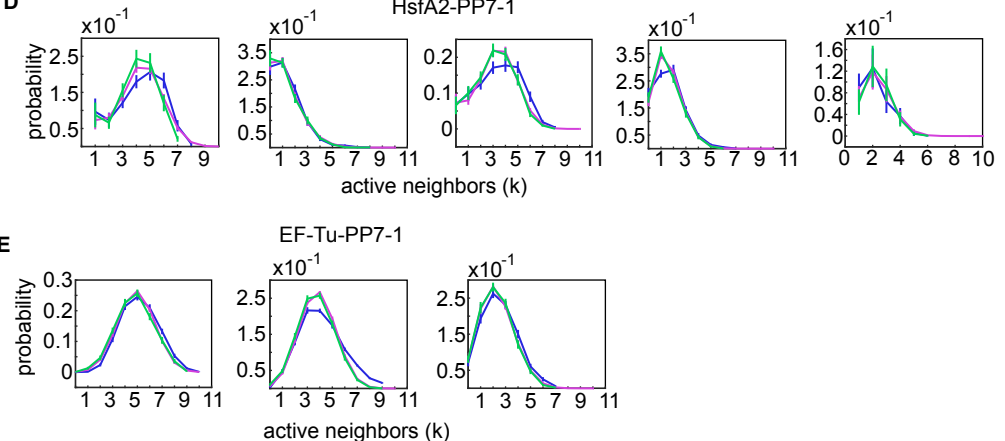
- active nucleus
- 4 inactive neighbors
- 1 active neighbor
- probability of active neighbors = 1/5



C



D



E

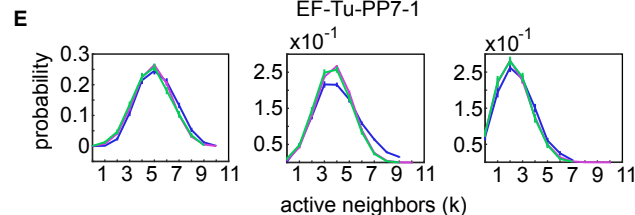


Figure S15. Related to Figure 3: Transcriptionally active nuclei are randomly distributed in space. (A)

The hypergeometric distribution describes the probability of finding k successes in a sample of size n drawn randomly from a population of size N with K total successes. If nuclei containing transcription spots are randomly distributed in space, the hypergeometric distribution would capture the probability of a nucleus having k active nuclei among its n closest neighbors given K total active nuclei in a field of view containing N nuclei. (B) Schematic showing how the formula in (A) is applied to nuclei in a field of view. Nuclei with spots are represented by dark green circles. Light green circles represent nuclei without spots. For each transcribing nucleus (dark green circle with magenta border), we calculate the probability of finding another active nucleus among its closest neighbors (also denoted by a black border). An experimental probability distribution of active neighbors is then built by repeating this operation for all active nuclei. Caption continues on next page.

Figure S15. Continued from previous page: Related to Figure 3: Transcriptionally active nuclei are randomly distributed in space. To build an experimental random distribution based on the data we randomize the positions of active nuclei and repeat this procedure. The random distribution can also be calculated analytically using the hypergeometric distribution in (A). (**C**) Probability distribution of the number of active neighbors (k) among the 10 closest neighbors (n) to each nucleus in the field of view of HSP101-PP7-1 replicates. Shown in magenta is the hypergeometric distribution (i.e., expectation if active nuclei are randomly distributed in space). In green is the distribution resulting from randomizing the position of actively transcribing nuclei. Actual experimental data is shown in blue. (**D**) Same as (C) for HsfA2-PP7-1 replicates. (**E**) Same as (C) for EF-Tu-PP7-1 replicates. Error bars in (C), (D), and (E) correspond to the SEM taken over $n = 43, 50$ and 83 frames, respectively. The spatial distribution of active nuclei is close to that of the randomized data and similar to the theoretical random expectation. Thus, we conclude that there is no evidence for spatial structure in the transcriptional state of nuclei in the field of view.

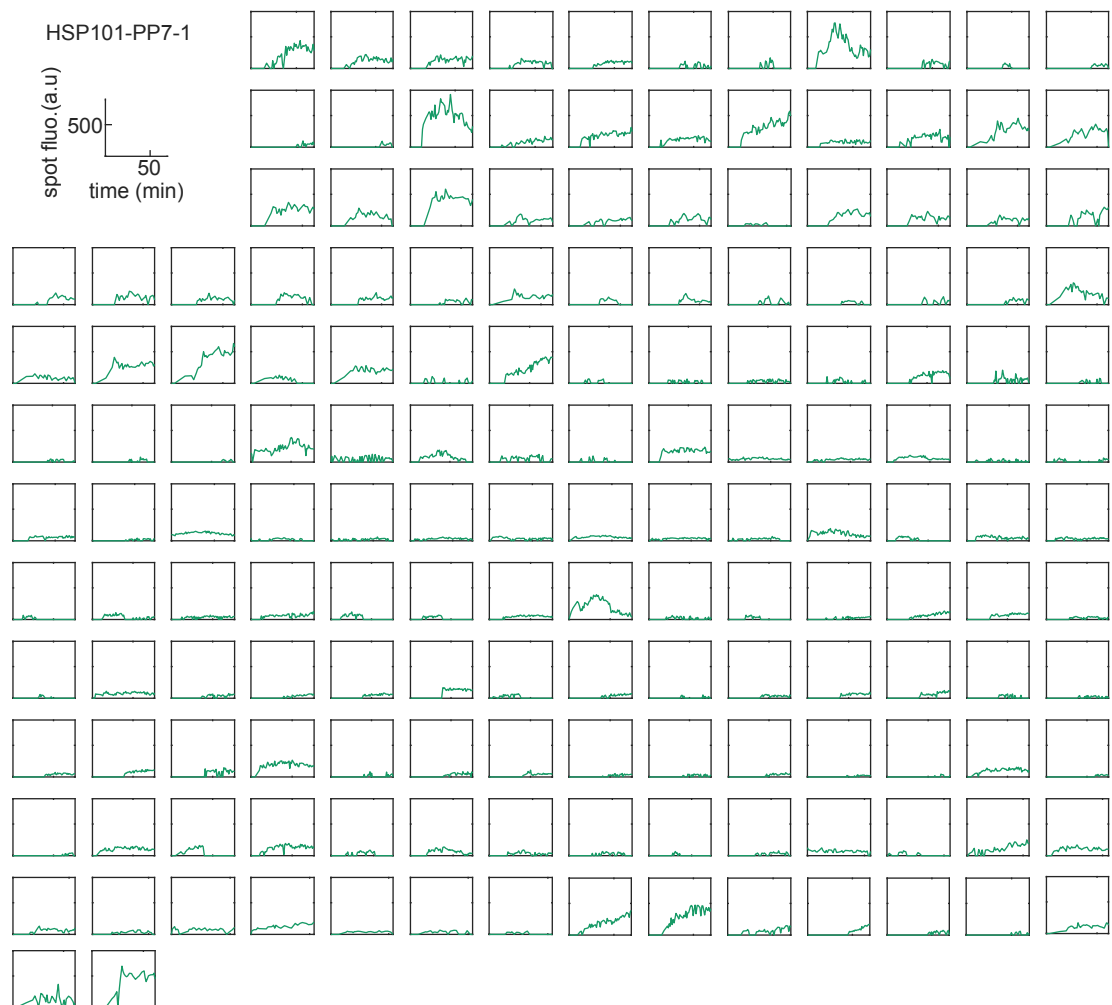


Figure S16. Related to Figure 3: Behavior of single loci in HSP101-PP7-1. Spot fluorescence time traces of individual loci in 8 replicates of HSP101-PP7-1 plants.

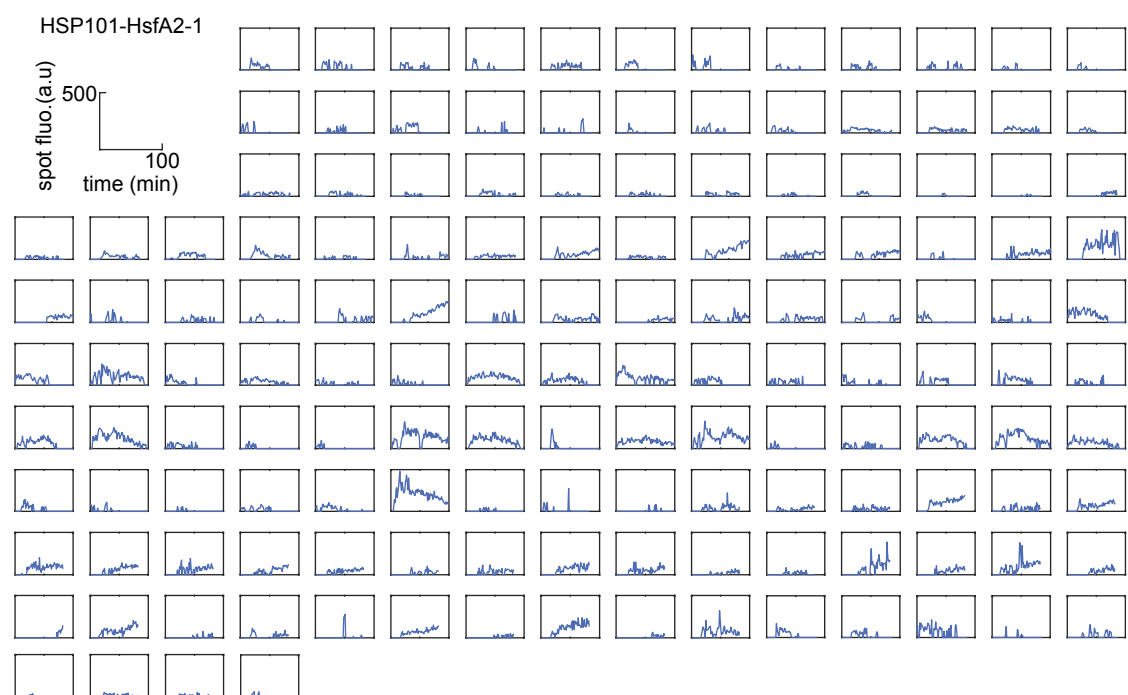


Figure S17. Related to Figure 3: Behavior of single loci in HsfA2-PP7-1. Spot fluorescence time traces of individual loci in 4 replicates of HsfA2-PP7-1 plants.



Figure S18. Related to Figure 3: Behavior of single loci in EF-Tu-PP7-1. Spot fluorescence time traces of individual loci in 3 replicates of EF-Tu-PP7-1 plants.

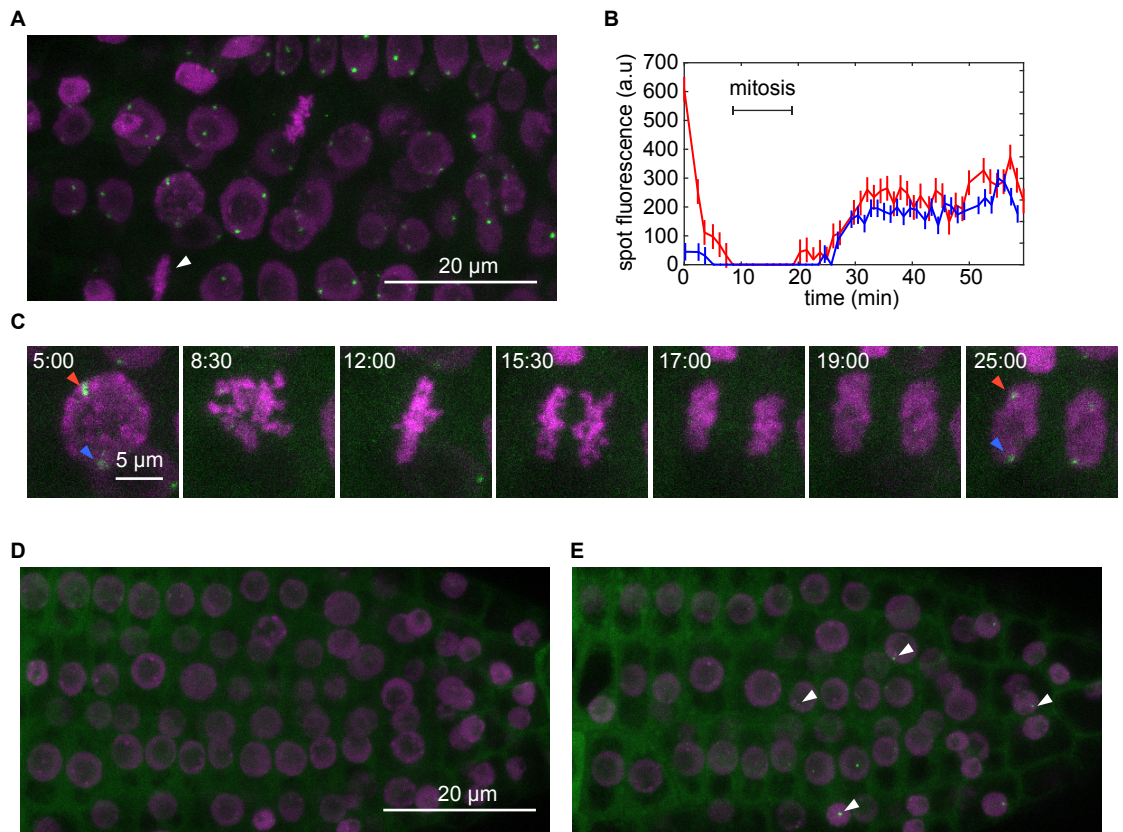


Figure S19. Related to Figure 3A. Imaging transcription in *Arabidopsis* roots. **(A)** Maximum projection snapshot of *Arabidopsis* root cells expressing H2B-mScarlet, PCP-GFP and EF-Tu-PP7. The white arrowhead indicates a cell undergoing mitosis. **(B)** Spot fluorescence before and after mitosis in the cell highlighted in (A). Each line corresponds to a different single transcription spot. Error bars correspond to the uncertainty in spot fluorescence calculation as described in the Materials and Methods. **(C)** Snapshots of the cell undergoing mitosis in (A). Red and blue arrowheads indicate the spots whose fluorescence is shown in (B). **(D)** Maximum projection snapshot of *Arabidopsis* root cells expressing H2B-mScarlet, PCP-GFP and HsfA2-PP7 at room temperature. **(E)** Same sample as in (D) after 30 min under a 39°C heat shock treatment. white arrowheads indicate transcription spots.

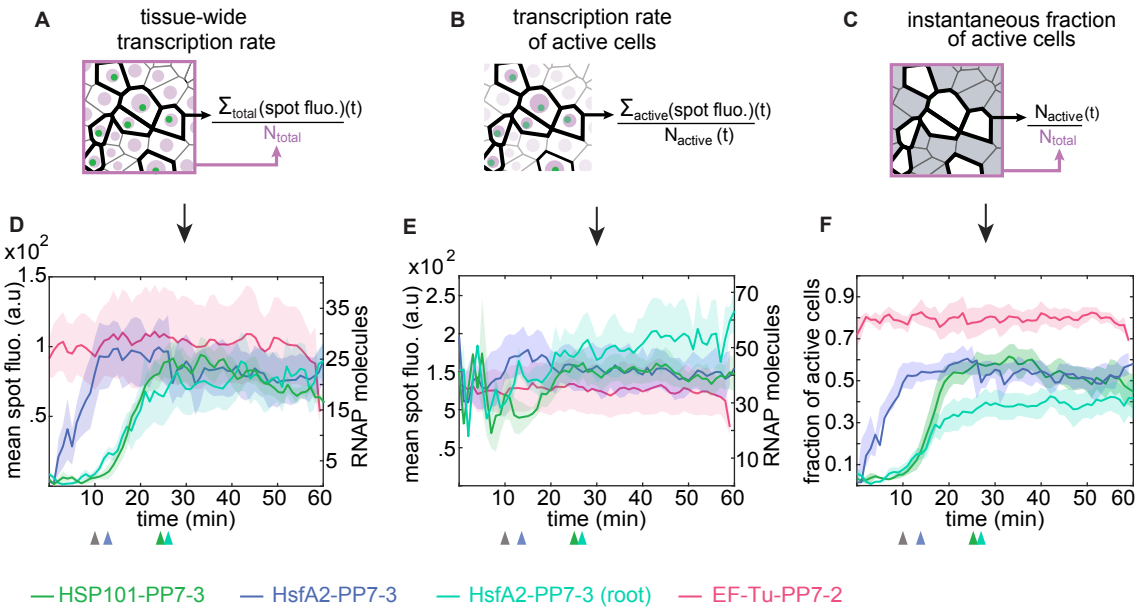


Figure S20. Related to Figure 5: Experimental replicates using different independent transgenic lines of each promoter construct. We repeated the experiments and analysis described in Figure 5 using different single-insertion transgenic lines carrying the same reporter constructs. **(A)** The tissue-wide transcription rate is calculated by adding the fluorescence of all spots in the field of view (\sum_{total}) in each frame and dividing by the total number of nuclei (N_{total}). **(B)** The transcription rate of active cells is calculated as in (A) except that the average is taken only over nuclei with spots in each frame ($N_{active}(t)$). **(C)** The instantaneous fraction of active nuclei corresponds to the number of nuclei exhibiting a spot in each frame divided by the total number of nuclei in the field of view. **(D)** Mean tissue-wide transcription rate in independent *Arabidopsis* transgenic lines carrying PP7 reporters driven by the promoters of HSP101, HsfA2 and EF-Tu as in Figure 5 inserted in different genomic locations. **(E)** Mean transcription rate of actively transcribing cells. **(F)** Mean fraction of active nuclei as a function of time. In (D-F) the shaded area corresponds to the SEM taken over n= 4, 4, 3 and 3 replicates for lines HSP101-3, HsfA2-3 (leaves), HsfA2-3 (roots) and EF-Tu-2, respectively. The arrowheads under each graph indicate the time points used to calculate the fold-change with respect to 10 minutes since the detection of the first spot (gray arrowhead). Because HsfA2-PP7-3 (blue) peaks near 10 minutes, 5 minutes were used for the fold change calculation of this dataset. These fold changes are shown in Figure 5H.

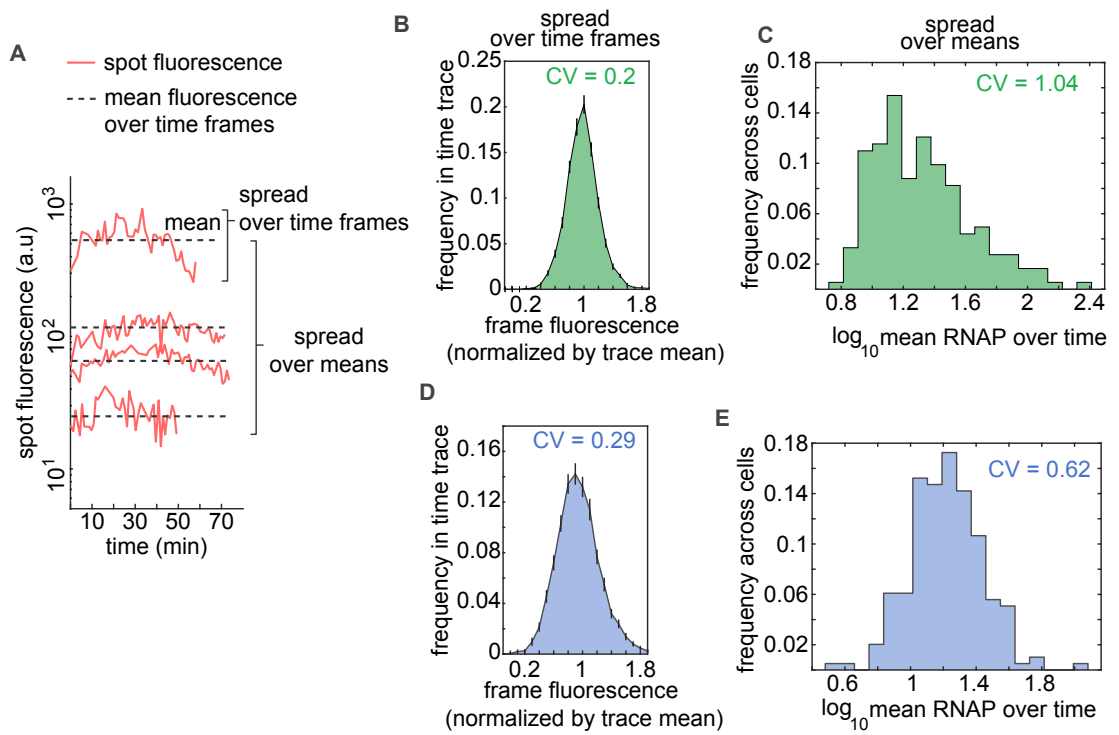


Figure S21. Related to Figure 5: Spot fluorescence varies widely across cells but is relatively stable over time in individual cells. (A) Representative spot fluorescence time traces in HSP101-PP7-1 replicates from Figure 3. Dashed lines correspond to the mean level of fluorescence of each trace taken over time. The spread of fluorescence values around this mean for each individual trace (“spread over time”) informs about temporal fluctuations in transcriptional activity for each individual spot. The variability of mean fluorescence values across cells is captured by the “spread over means” and informs about cell-to-cell heterogeneity in activity. (B) Spread over time revealed by the distribution of frame fluorescence values normalized by the mean over time for each fluorescence trace pooled from all HSP101-PP7-1 replicates from Figure 3. The spread over time of fluorescence values of a given spot is very close to the mean, resulting in a coefficient of variation (CV=standard deviation/mean) of 0.2. (C) spread over means as reported by the distribution of mean fluorescence over time (see dashed lines in (A)) of all cells in HSP101-PP7-1 replicates. The average transcriptional activity varies widely across cells, with a coefficient of variation of 1.04. (D,E) Same as (B) and (C) for HsfA2-PP7-1 fluorescence traces pooled across replicates from Figure 5. Error bars in (B) and (D) correspond to the standard error over n= 8 and n= 5 biological replicates.

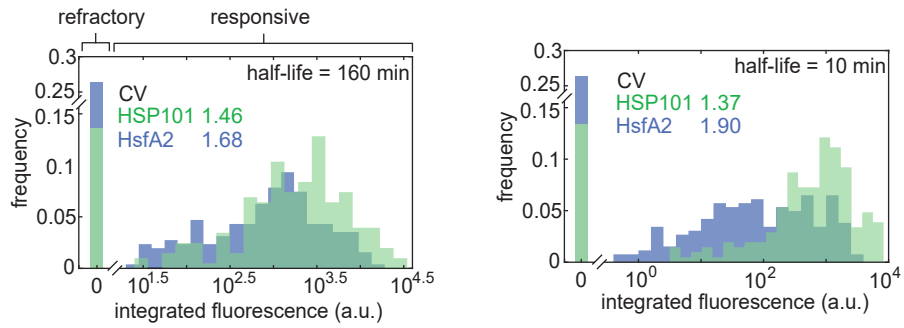


Figure S22. Related to Figure 6B: Distribution of accumulated mRNA taking degradation into account.

Histograms showing the distribution of accumulated mRNA per cell in all pooled replicates of HSP101-PP7-1 and HsfA2-PP7-1 shown in Figure 3 as in Figure 6B. Two different mRNA half-lives were simulated, a realistic one of 160 minutes and very short one of 10 minutes. The value of 160 minutes was determined by fitting the RT-qPCR signal in Figure S7E. The calculation of accumulated mRNA based on spot fluorescence data is based on the assumptions described in Figure S5 and calculated as described in Section S1.1. The coefficients of variation (CV = standard deviation/mean) with a half-life of 160 minutes are virtually identical to those in Figure 6B obtained with an infinite half-life. The CV values are qualitatively similar even with an unrealistically short half-life of 10 minutes.

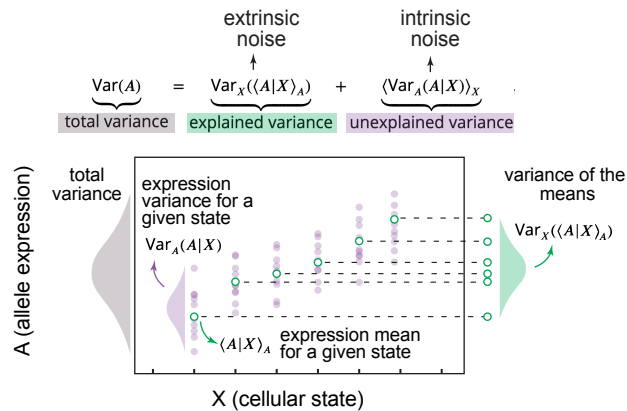


Figure S23. Related to Figure 6 and calculations in Section S1.4: Visual explanation of the law of total variance. Shown as a gray distribution on the left of the graph is the total variance in the expression of a gene (A) in a population of cells which varies depending on the cellular state (X). The total variance is composed of two types of variance, explained and unexplained, corresponding to extrinsic and intrinsic noise, respectively. As depicted by the green distribution to the right of the graph, subpopulations of cells belonging to different states will have different mean values of A since A depends on X. This variance is explained by the value of X being shared across cells within a subpopulation but different across different subpopulation and is thus referred to as explained variance. On the other hand, cells in an identical state X can still have variable values of A (purple distribution). Since these cells share the same value of X, their variance is not explained by differences in cellular state. Thus, this intra-state variability is referred to as unexplained variance. .

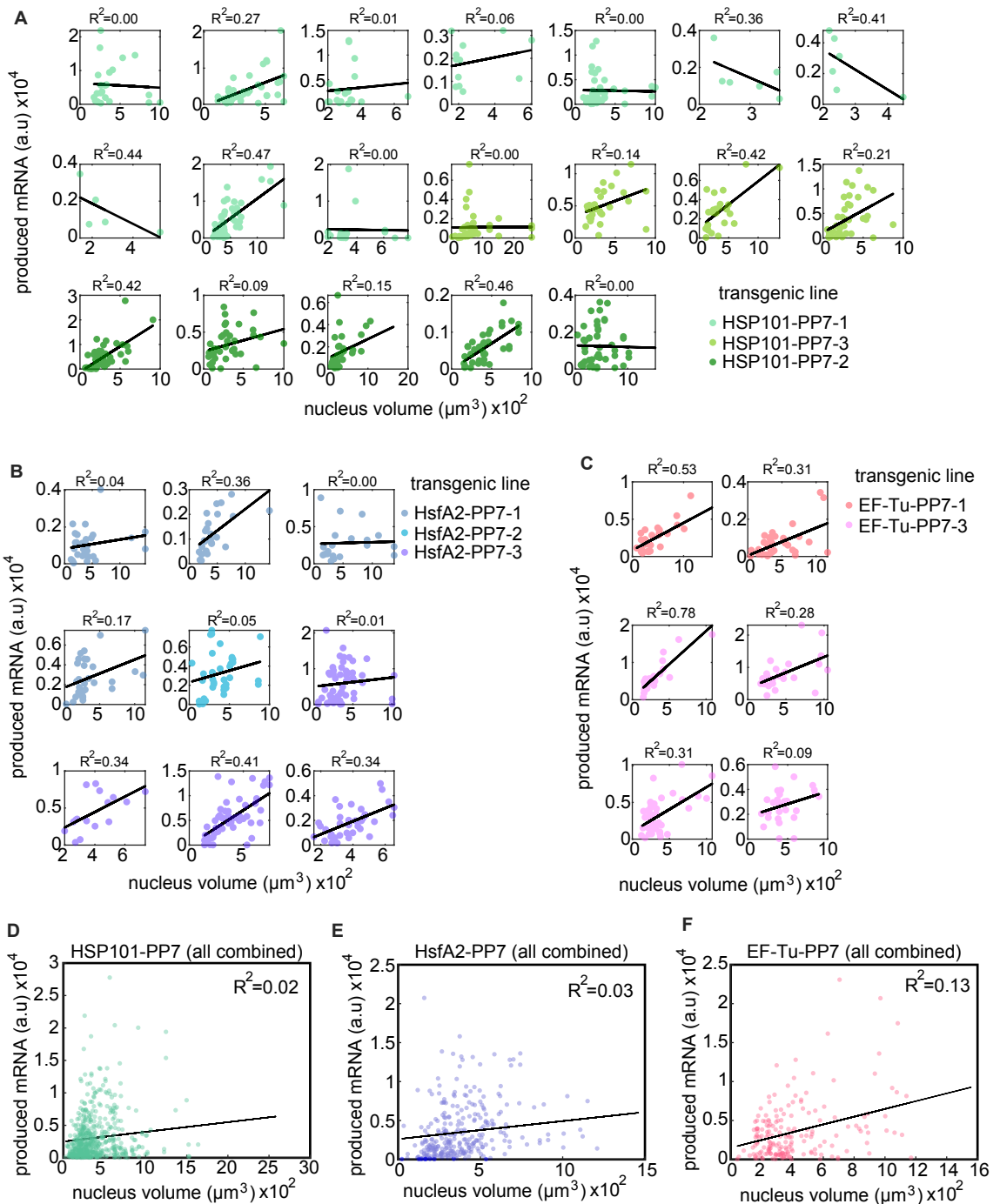


Figure S24. Related to Figure 6: Nucleus volume is positively but only weakly correlated with transcriptional output. (A-C) In each movie, nuclei were segmented at a single frame at ≈ 30 minutes based on Histone-mScarlet using the ImageJ Weka machine learning toolbox [?]. To calculate their volume, nuclei were fitted to an ellipsoid based on the length of their major and minor axes. If a nucleus contained a transcription spot, its produced mRNA (calculated as integrated fluorescence over time) is plotted against its corresponding nuclear volume as a scatter plot. If a nucleus contained two transcription spots, as in the case of homozygous individuals, the integrated fluorescence of spots was averaged. Black lines on top of each scatter plot show the best fit to the data based on a linear model. The coefficient of determination (R^2) is shown on top of each plot. (D-F) Same as (A-C) except that nuclei from all replicates and transgenic lines were pooled together for each reporter construct.

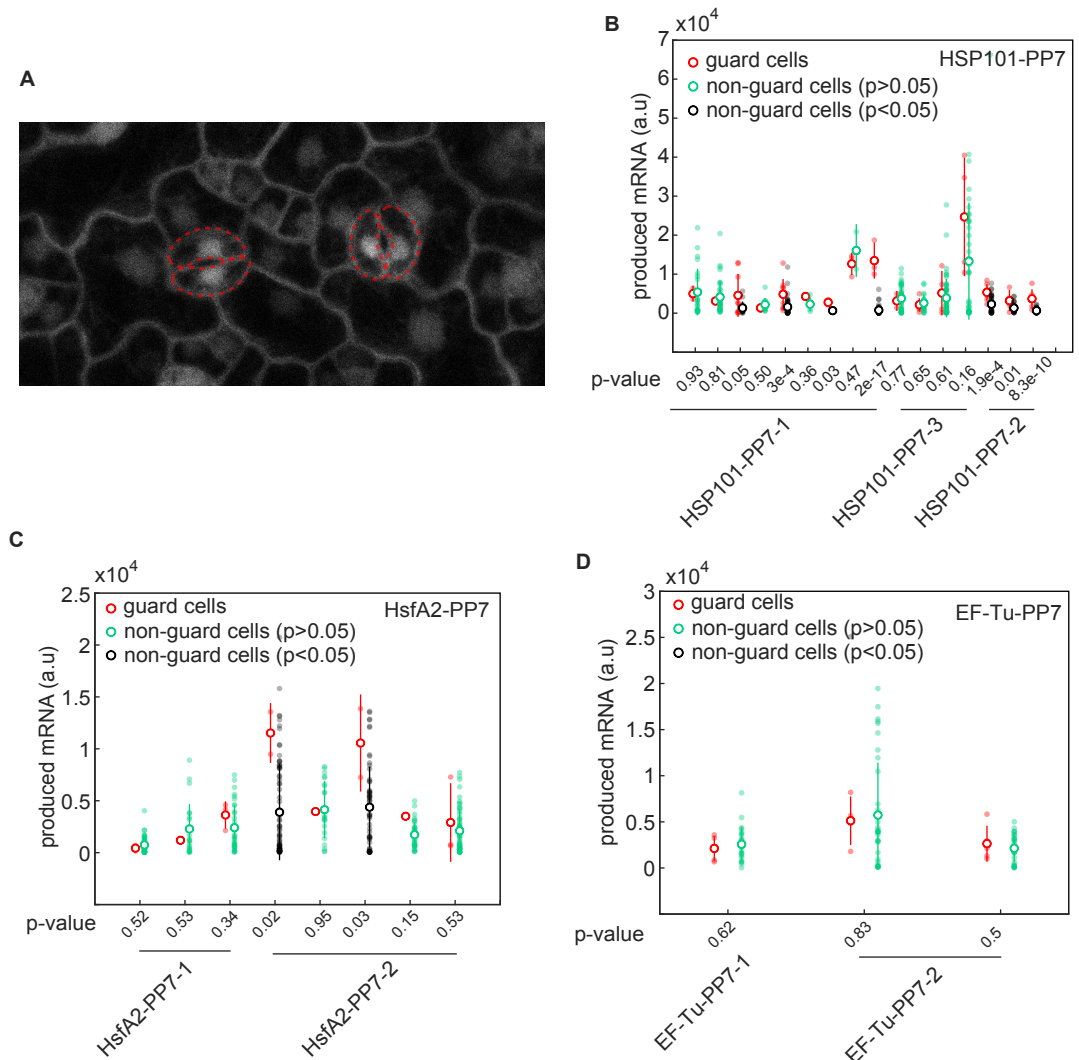


Figure S25. Related to Figure 6: Guard cells do not consistently transcribe at different levels than the rest of cells. (A) Arabidopsis epidermis cells expressing PCP-GFP. Dashed red lines highlight guard cells. (B-D) In each movie of each line presented in this study, the mean total mRNA produced by guard cells (red) was compared to that of non-guard cells. A two-sided t-test was used to determine if guard cells are statistically different than the rest of cells. Non-guard cells are plotted in black if the test p-value is lower than 0.05 and in green otherwise, showing that guard cells do not transcribe at a different level in a consistent manner. Only replicates in which guard cells were present are shown. Error bars in (B), (C), and (D) correspond to the standard deviation across nuclei in the field of view. Open circles correspond to the mean across nuclei in the field of view. The number of cells (n) in each replicate corresponds to the number of filled circles.

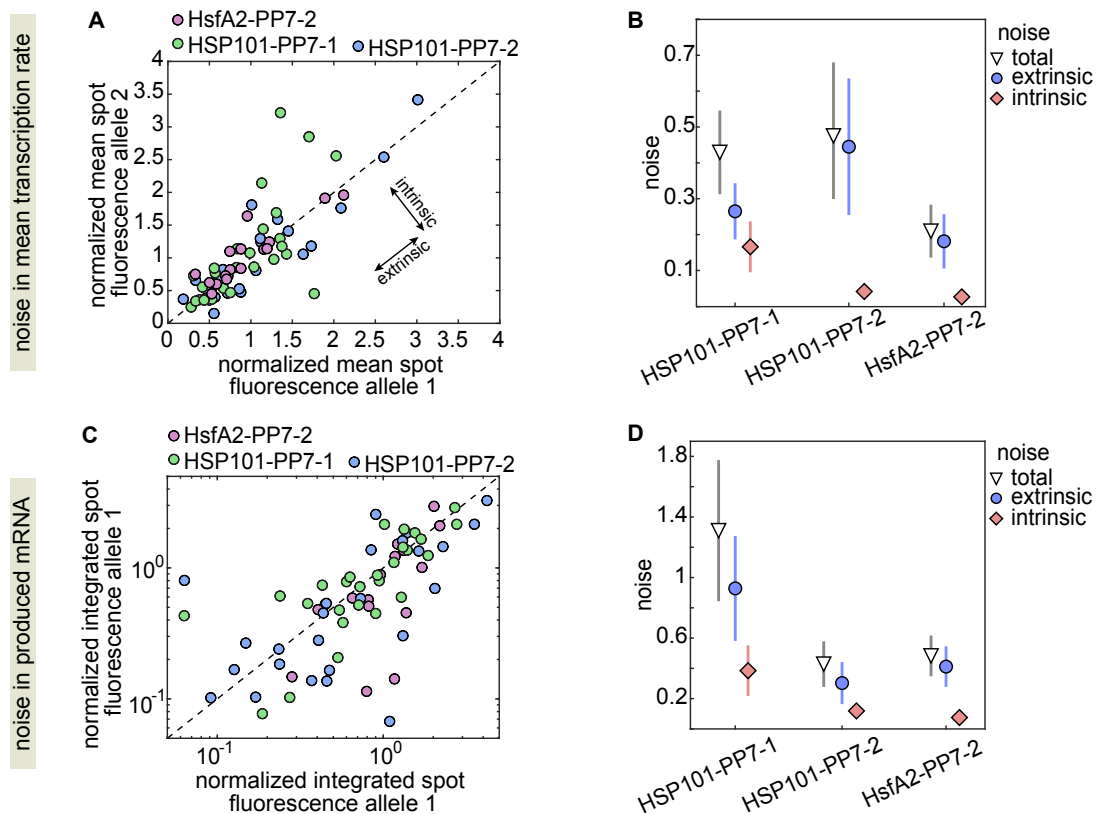


Figure S26. Related to Figure 6: Extrinsic noise is larger than intrinsic noise among nuclei with two active alleles. **(A)** Scatter plot showing the mean spot fluorescence over time for allele pairs belonging to the same nucleus in three different single-insertion lines homozygous for the PP7 reporter. **(B)** Decomposition of the total variability in (A) into its intrinsic and extrinsic components. **(C)** Scatter plot of integrated fluorescence over time in allele pairs belonging to the same nucleus in three different single-insertion reporter lines homozygous for the PP7 transgene (same as Figure 6E except that inactive alleles are not included). **(D)** Decomposition of the total noise in (C). In (A) and (C) values were normalized to the mean across all alleles in that line and the diagonal line shows $y=x$. Error bars in (B) and (C) correspond to the bootstrapped error (1000 samples) taken over 128, 111, and 69 nuclei obtained from two biological replicates of HSP101-PP7-1, HSP101-PP7-2 and HsfA2-PP7-2, respectively..

1015 **S4 Supplementary Videos**

- S1. [Video 1. Constitutive reporter in tobacco.](#) Movie of tobacco cell expressing PCP-GFP and GACP2-PP7. The scale bar is 10 μm .
- S2. [Video 2. Inducible reporter in tobacco.](#) Movie of tobacco cell expressing PCP-GFP and HSP70-PP7 under heat shock treatment starting at 10 min. The scale bar is 10 μm .
- 1020 S3. [Video 3. Inducible HSP101-PP7 reporter in Arabidopsis tissue.](#) Movie of leaf cells in Arabidopsis line stably transformed with PCP-GFP and HSP101-PP7 under heat shock treatment starting at 6 min. The scale bar is 10 μm .
- S4. [Video 4. Inducible HsfA2-PP7 reporter in Arabidopsis tissue.](#) Movie of leaf cells in Arabidopsis line stably transformed with PCP-GFP and HsfA2-PP7 under heat shock treatment starting at 8 min. The scale bar is 10 μm .
- 1025 S5. [Video 5. Constitutive reporter in Arabidopsis tissue.](#) Movie of leaf cells in Arabidopsis line stably transformed with PCP-GFP and EF-Tu-PP7. The scale bar is 10 μm .
- S6. [Video 6. Arabidopsis plant homozygous for an inducible reporter.](#) Movie of leaf cells in a homozygous Arabidopsis line stably transformed with PCP-GFP and HSP101-PP7 under a heat shock treatment starting at 0 min. The scale bar is 10 μm .
- 1030